Feature Extraction Techniques for Noisy Distributed Acoustic Sensor Data Acquired in a Wellbore

JAGADEESHWAR TABJULA,[1] AND JYOTSNA SHARMA[1,*]

[1]Department of Petroleum Engineering, Louisiana State University, Baton Rouge 70803, USA
*jsharma@lsu.edu

Abstract: Distributed acoustic sensor (DAS) is a promising technology for real-time monitoring of wellbores and other infrastructures. However, the desired signals are often overwhelmed by background and environmental noise inherent in field applications. We present a suite of computationally inexpensive techniques for the real-time extraction of gas signatures from noisy DAS data acquired in a 5163-ft-deep wellbore. The techniques are implemented on three well-scale DAS datasets, each representing multiphase flow conditions with different gas injection volumes, fluid circulation rates, and injection methods. The proposed denoising techniques not only helped in optimizing the gas slug signature despite the high background noise, but also reduced the DAS data size without compromising the signal quality.

1. Introduction

Optical fiber-based distributed acoustic sensors (DAS) are considered a promising technology for real-time monitoring because of their ability to provide distributed acoustic or vibration measurements simultaneously along the entire length of the installed fiber at a high spatial and temporal resolution [1]. In recent years, they have gained increasing popularity in the petroleum industry for the monitoring of wellbores and reservoirs owing to their many advantages over traditional surveillance methods [2]. They are lightweight, chemically passive, immune to electromagnetic influence, and do not require any electronics along the optical path [3]. However, owing to their high sensitivity, DAS signals are often overwhelmed by environmental noise inherent to the dynamic and harsh downhole conditions in a wellbore [4]. Thus, signal processing and denoising techniques are necessary for extracting the signatures of interest from the background noise. Additionally, DAS generates large volumes of streaming data due to the data acquisition at high spatial and temporal frequency. This can result in data size in the order of terabytes per day, for an average well length. Since many oil fields operate in remote locations with limited bandwidth, processing, storing, and interpreting voluminous DAS data in real-time can be difficult. To address these challenges, this study presents a suite of computationally inexpensive signal processing techniques for extracting the signals of interest from noisy DAS measurements in real-time, while also addressing the voluminous data handling issues.

The workflows are demonstrated on DAS datasets acquired during multiphase flow tests in a 5163-ft-deep wellbore. The goal was to optimize the detection and visualization of gas (nitrogen) bubbles through a rapidly circulating column of wellbore fluid (water) in real-time. These tests were aimed at mimicking well control conditions that arise when an unwanted influx of formation gas (also known as a “kick”) enters the wellbore during workover, drilling, or completion operations. If not detected and mitigated in time, the unloading of gas influx at the surface can lead to blowout conditions that can result in ecological and economic disaster [5]. Traditional kick detection/monitoring technologies rely primarily on surface-based measurements, which might be insufficient for real-time monitoring due to their latency and limited spatial resolution [5,6]. Fiber-optic sensors can overcome these limitations by providing data across the entire length of the installed fiber on a wellbore and/or drilling riser to inform gas kick location in real-time [7-9]. Three DAS datasets are analyzed in this study, each representing different gas influx volumes, fluid circulating conditions, and gas injection methods in well-scale settings. The efficacy of the different denoising techniques to optimize gas detection is illustrated using both the raw and processed DAS data. The effect of DAS acquisition parameters, such as gauge length and time frame, on the signal quality, is also evaluated using the experimental data.

2. Experimental Setup

The data analyzed in this work was acquired at the Petroleum Engineering Research, Training, and Testing (PERTT) lab at Louisiana State University (LSU) in a 5,163-ft-deep wellbore. The test well (Fig. 1a) has a cemented casing of 9.625 in. outer diameter (OD) and a production tubing of 2.875 in. OD to a depth of 5025 ft. The DAS measurements were obtained using a single-mode fiber that was pumped in an optical control line strapped to the outside of the production tubing using steel clamps. Fig. 1d shows the schematic of the wellbore, including the casing and tubing dimensions, along with the optical interrogator connected to the wellbore fiber at surface. For all tests, the length of the fiber under test is 5,025 ft (1.53 km) in the well. In addition to the fiber-optic sensor, the well is also instrumented with downhole temperature and pressure gauges, surface flowmeters, and adjustable chokes to regulate the back pressure.

A series of multiphase flow experiments were conducted in the well to study gas migration dynamics in static and circulating wellbore fluid. DAS data from three experimental tests are analyzed in this study that represent different gas (nitrogen) influx volumes, fluid (water) circulation rates, and gas injection conditions, as summarized in Table 1. Commercially available optical interrogator units were used for the DAS acquisition that combine the Rayleigh backscattered light from the single-mode fiber with a local oscillator in a heterodyne process to extract the optical phase from the signal. The measurement specifications for DAS acquisition are summarized in Table 2. Trials 1 and 2 utilize a DAS interrogator that stores the acquired vibration data in the form of strain rate with a fixed gauge length. For Trial-3, a different interrogator was used that stores the velocity profile across the fiber which can be converted to strain rate in post-processing using a desired gauge length [10].

The experiments are schematically represented in Figs. 1b through 1d, where the orange color indicates the nitrogen gas slug, blue color indicates the wellbore fluid (water), and the orange and blue arrows indicate the direction of gas displacement and water circulation, respectively. In the first trial (Fig. 1b), a small quantity (2 barrels or bbl) of gas was injected into the tubing and allowed to migrate into the water-filled annulus while the pump was turned off. The resulting DAS data was free of the pump and circulating fluid noise and therefore used as a baseline for comparison with the relatively nosier data from the other two trials where water was pumped at high rates. Real oilfield applications are seldom devoid of pump noise because fluid circulation accompanies production, injection, and drilling operations. To account for this, in the other two trials (Trial-2 and Trial-3), gas displacement was monitored while the wellbore water was circulated at high rates. In Trial-2 (Fig. 1c), the gas influx was simulated by injecting 15 bbl of nitrogen gas slug down the tubing and subsequently displacing it by circulating water at 200 gallons per minute (gpm) volumetric flow rate. Water circulation is continued for the entire duration of the trial until the gas is completely removed from the wellbore annulus to the surface. In the final trial (Trial-3), a much larger nitrogen gas slug of 80 bbl was injected from the annulus side to simulate a “gas below BOP (blowout preventer)” scenario (Fig. 1d). Once the gas injection stopped, the well system was given some time to equilibrate, resulting in the expansion of the injected gas cap. Subsequently, the gas column was pushed down through the annulus with water at 250 gpm rate while taking returns from the tubing with the choke fully open. In comparison to Trial-1, the DAS data obtained in Trials 2 and 3 were impacted by the vibrations due to the pump and fluid circulation noise and therefore required additional signal conditioning and denoising to optimize gas slug detection.

The resulting DAS data was used to monitor the precise position of the top and bottom of the gas slug region in the wellbore in real-time, as conventional point sensors and gauges lack this ability. This information is used to track the changing gas slug lengths as well as the influx velocity as the gas-liquid mixture travels across the annulus and predict the time of arrival of gas at surface. These parameters ultimately dictate the well control procedure needed to manage the kick and prevent blowout incidents. The gas slug lengths and displacement velocities vary across the wellbore due to the changing pressures and hence the dynamic multiphase displacement behavior needs to be closely monitored.

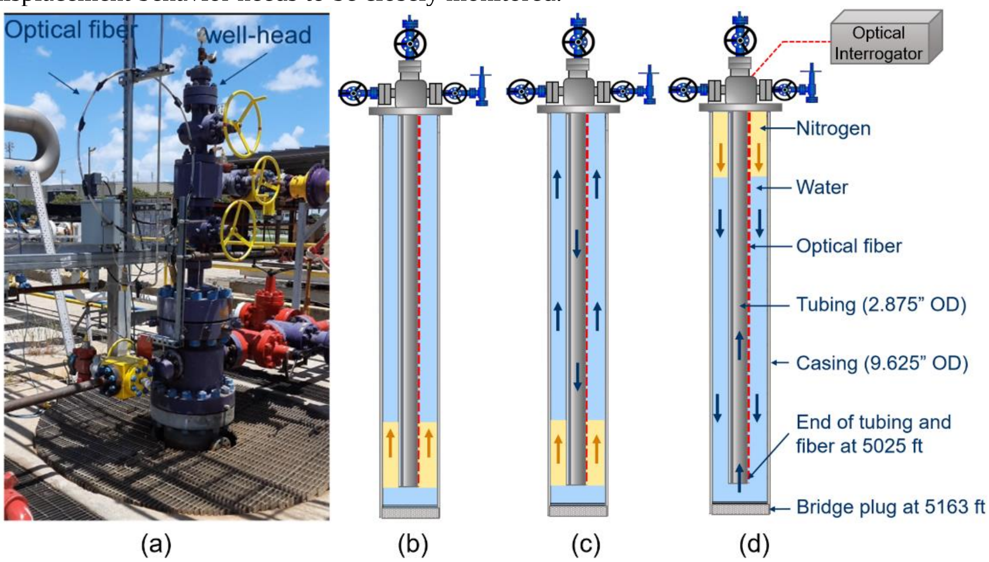

Fig. 1. (a) Test well used in the study. Schematics of multiphase flow condition during (b) Trial-1 (c) Trial-2 (d) Trial-3. For all the trials, the length of the fiber under test is 5,025 ft (1.53 km).

Table 1. Operating conditions during the three experimental trials.

Trial	Injection volume (bbl)	Initial gas location in the annulus	Pump rate (gpm)	Direction of water flow	Direction of gas displacement
1	2	Bottom	0	No water flow	Up the annulus
2	15	Bottom	200	Down the tubing and up the annulus	Up the annulus
3	80	Top	~250	Down the annulus and up the tubing.	Down the annulus

Table 2. Measurement specifications of the DAS interrogator unit (IU) used during the three trials.

Parameter	IU Specifications for Trials 1 and 2	IU Specifications for Trial-3
Optical fiber	Single-mode	Single-mode
Range	9.94 miles (16 km)	4.97 miles (8 km)
Spatial resolution	4.92 ft (1.5 m)	16.07 ft (4.9 m)
Sampling interval	2.53 ft (0.77 m)	8.03 ft (2.45 m)
Sampling frequency	10 kHz	4 kHz

3. Methodology

This section explains the different signal processing techniques that were implemented on the DAS data to optimize the detection and visualization of gas displacement during the experimental trials. The raw DAS vibration data is obtained in the form of strain rate information as a function of time at any given location along the fiber. The amount of additional signal processing required for a given spatial-temporal DAS vibration data depends on the clarity of the signal (or feature) of interest. Ten-second frames of DAS vibration data for Trials 1, 2, and 3 are shown in Fig. 2. The gas signature (including the top and bottom of the gas slug region which becomes a two-phase gas-liquid mixture in the well) is clearly visible in the static water column and annotated for Trial-1 in Fig. 2a. However, for Trials 2 and 3, despite the larger amount of injected gas slug, the gas signature cannot be identified because the signal is buried in the tmp and flow noise due to the high water circulation rates. Hence, there is a need for further signal conditioning and denoising to optimize the gas feature detection.

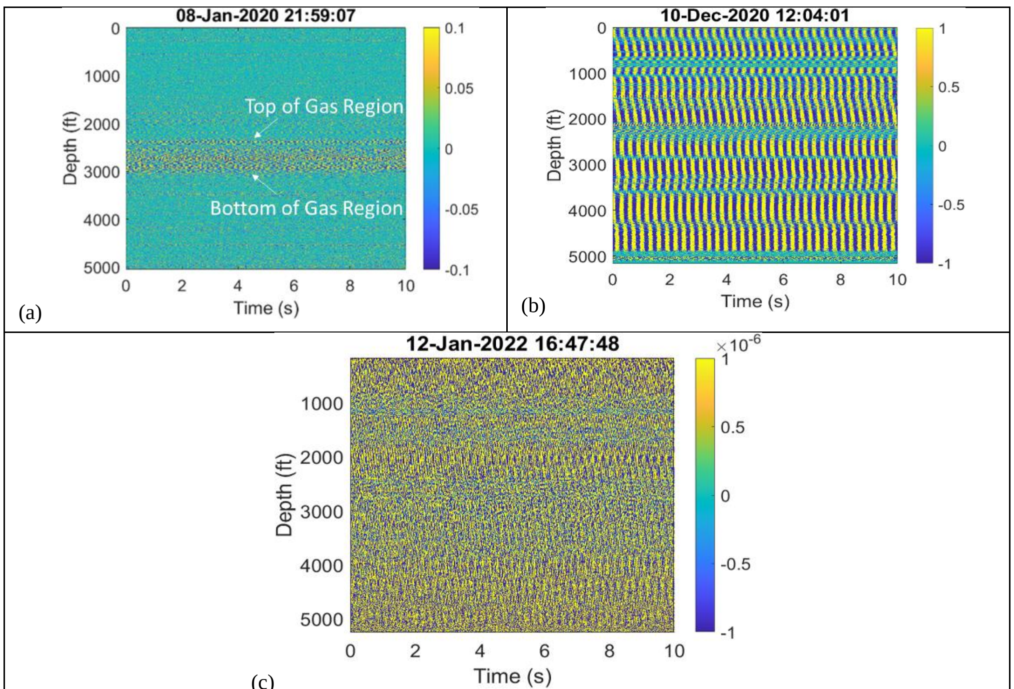

Fig 2. Sample ten-second time frames of raw DAS vibration data for (a) Trial-1 where the top and bottom of the gas slug region are clearly visible (b) Trial-2 and (c) Trial-3.

A suite of computationally inexpensive real-time implementable signal processing and denoising techniques are described below. These methods not only improve the signal quality, but also reduce the DAS data storage needs. Depending on the amount of background noise and level of signal distortion, one or more of these methods can be utilized.

(a) **Mean**

Starting with one of the most basic techniques, a moving average or mean is calculated on the DAS time-series data. Signal averaging can help in reducing the noise without compromising details [11]. Consider the raw DAS strain rate or vibration data expressed as K time frames and each time frame represented as $Q \in \mathbb{R}^{DXT}$, where D and T are the numbers of the samples in the space and time dimensions, respectively. Mean is computed on each time frame using Eq. (1). and the computed mean across all the K time frames is stored as a single matrix as M^{DXK}.

$$A = \frac{\Sigma_{t=1}^{T} Q_{dt}}{T} \in \mathbb{R}^{DX1} \quad \text{.......................................} (1)$$

(b) **Standard deviation**

Standard deviation is another computationally inexpensive technique that can help in enhancing the signal-to-noise-ratio (SNR), especially for dynamic processes. Standard deviation of each time frame is computed using Eq. (2). This can be calculated for all the time frames and appended as STD^{DXK}.

$$S_{DX1} = \sqrt{\frac{1}{T-1}\Sigma_{i=1}^{T}|Q_{di} - A_d|^2} \ldots\ldots\ldots\ldots\ldots\ldots\ldots\ldots\ldots (2)$$

(c) **Root mean square (RMS)**

Another treatment that is simple to execute in real time is the RMS, which can be derived using Eq. 3 and the resulting outcomes of different time frames can be stored in a single matrix as RMS^{DXK}. This method can help in smoothing out rapidly changing signals, such as noise [12].

$$R = \sqrt{\frac{\Sigma_{i=1}^{T}|Q_{di}|^2}{T}} \in \mathbb{R}^{DX1} \ldots\ldots\ldots\ldots\ldots\ldots\ldots\ldots\ldots (3)$$

(d) **Frequency band energy (FBE)**

FBE is a powerful signal processing technique that not only reduces the DAS data storge space but also reduces the noise by filtering the desired frequency range [2]. Fast Fourier transform (FFT) is applied to the time-series data, and the resultant magnitude is denoted as $H \in \mathbb{R}^{DXF}$ where D and F are the same numbers of samples in Q, but in the space and frequency dimension. Then FBE is calculated as $G = \Sigma_{i=f_l}^{f_h} H_{di}^2 \in \mathbb{R}^{DX1}$ where f_l, and f_h are lower and higher cut-off frequencies of the selected frequency band range. Subsequently FBE is calculated for all the K time frames and the resultant is denoted as $FBE^{[f_l - f_h]} \in \mathbb{R}^{DXK}$

(e) Fourier space filtering

Implementation of averaging or filtering can sometimes result in undesired horizontal or vertical bands in the processed signal. These bands may also be present inherently present in fiber-optic sensor data due to the non-uniform fiber coupling. One method to remove these is using 2D-FFT filtering. Let's consider the processed DAS data using the above-mentioned techniques be denoted as $C \in \mathbb{R}^{DXK}$. This data matrix can be converted into Fourier space using 2D-FFT and labeled as $E \in \mathbb{C}^{WXY}$, where W and Y are same number of elements in Fourier space as D and K. The frequency components which contribute to the noisy bands (such as the DC components which are close to the origin) can then be replaced with zeros and transformed back to space and time domain.

(f) Gradient filter

This filter computes the gradient depending on the appearance of the bands. If the noisy bands are on the time axis of C, then the gradient with respect to time is computed as shown as Eq 4 and labeled as $P \in \mathbb{R}^{DXK-1}$. If noisy bands are dominant in the depth axis, gradient is computed using Eq 4 but in-depth direction and labeled as $P \in \mathbb{R}^{D-1XK}$.

$$P_{d,i-1} = C_{d,i} - C_{d,i-1} \ \forall \ i = 2,3,4 \ldots . K \ldots\ldots\ldots\ldots\ldots\ldots (4)$$

(g) Gradient-based iterative destriping algorithm (GBDIA)

In this technique, a gradient mask is used to filter the noisy image or data matrix in the Fourier space by doing element wise matrix multiplication with the generated gradient mask. The data is then converted back to the space and time domain. GBDIA has been deployed for successfully destriping the satellite images [13].

Gradient mask is generated by first creating a matrix called $TEMP \in \mathbb{R}^{DX\frac{K}{2}}$ using Eq. 5. The matrix is then flipped horizontally and appended to its original as shown in Eq. 6 and labeled as $FI \in \mathbb{R}^{DXK}$.

$$TEMP_{ij} = \frac{(j-1)}{K} \in \mathbb{R}^{DX\frac{K}{2}} \ldots\ldots(5)$$

where $i = 1, 2, 3, \ldots D$ and $j = 1, 2, 3, \ldots \frac{K}{2}$.

$$FI = \left[TEMP\ TEMP_{d\left(\frac{K}{2}-1+j\right)}\right] \in \mathbb{R}^{DXK} \ldots\ldots(6)$$

where $j = 1, 2, 3, \ldots \frac{K}{2}$

A new matrix $WI \in \mathbb{R}^{DXK}$ is created by implementing equation 5 and 6 but in the column direction. . Then the gradient mask is computed using Eq. 7 and 8 where $tol \in \mathbb{R}$ is a tuning parameter.

$$GM = \left[\frac{FI \odot FI}{(FI \odot FI)+(WI \odot WI)+tol}\right] \in \mathbb{R}^{DXK} \ldots\ldots(7)$$

$$GM(GM > tol) = tol \ldots\ldots(8)$$

Here GM is computed by assuming noisy bands are in the horizontal direction. If noisy components are in vertical direction, Eq 7 can be written as:

$$GM = \left[\frac{WI \odot WI}{(FI \odot FI)+(WI \odot WI)+tol}\right] \in \mathbb{R}^{DXK}$$

4. Results and Discussion

4.1 Trial-1

Trial-1 was conducted by allowing gas migration in the annulus without water circulation. The raw DAS strain rate data of a single time frame (10 seconds) was shown in Fig. 2a. The location of the gas can be easily identified as there was minimal background noise due to no water circulation. However, the raw DAS data requires a large amount of storage space. Therefore, in order to enhance the signature, while reducing the data storage requirement, simple filtering and averaging techniques (a)–(c) described in Sec. 3, were applied to the DAS data acquired in Trial-1. A time frame (or frame size) of 10 seconds and gauge length of 4.92 m (fixed in the interrogator) were used for DAS processing, and the results are shown in Fig. 3. The gas signature, including the top and bottom of the gas displacing in the annulus at any given time, are clearly visible using all three methods. As previously mentioned, these techniques not only improve the signal but also minimize data storage space. For example, in Trial-1, each time frame of raw DAS strain rate data requires 897 MB of storage space, and Trial-1 has a thousand-time frames, occupying 875 GB. After converting to one of the aforementioned profiles, data storage space is reduced to 17.2 MB, a substantial decrease in size without significantly compromising the gas signature quality.

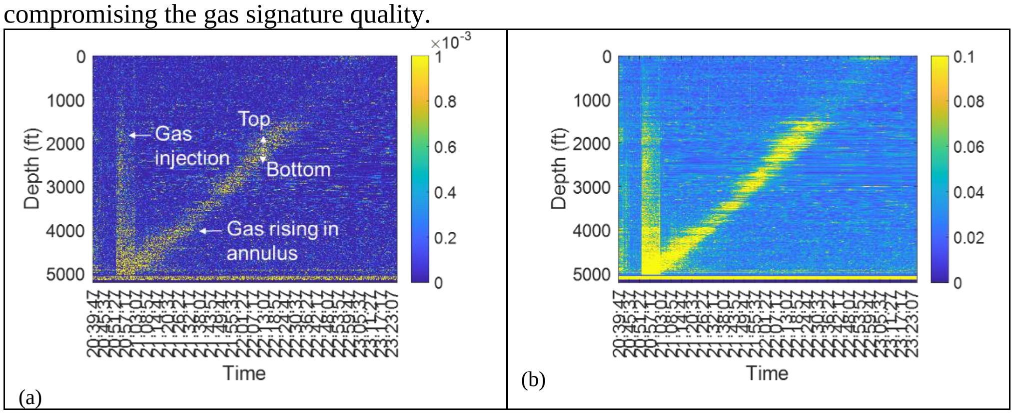

(a) (b)

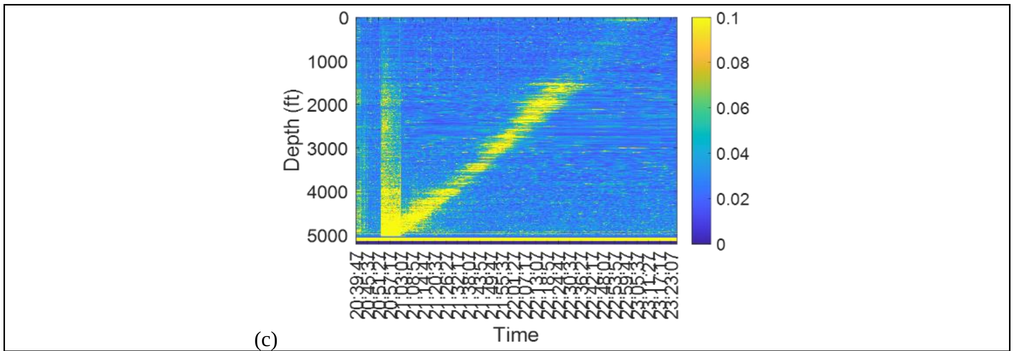

Fig. 3. Processed DAS data for Trial-1 using (a) mean (b) standard deviation (c) RMS. The figures show gas injection and gas rise signature including the top and bottom of the moving gas slug region at any given time.

Trial-1 data was also used to select the optimum frequency bands for visualizing the gas signature. The spectral signatures of gas displacement at different time instances for different depths are plotted in Figs. 4a-4d. The results demonstrate that the spectral signature of gas is dominant in the 0 to 50 Hz frequency range, as indicated by the high amplitude obtained in the spectrum plots. However, 10 to 50 Hz was selected as the optimum frequency band to visualize gas to avoid the DC noise at the lower frequencies. The FBE for the 10 to 50 Hz frequency band is computed for Trial-1 and shown in Fig. 4e. The gas rise signature, including the top and bottom of the gas slug region, is clearly observed across the entire wellbore annulus in this frequency range. Thus, this FBE represents the optimum frequency band corresponding to the gas displacement in the annulus of the test well. This information will be leveraged for processing the noisier DAS data acquired in Trials 2 and 3 that involve high fluid circulation rates.

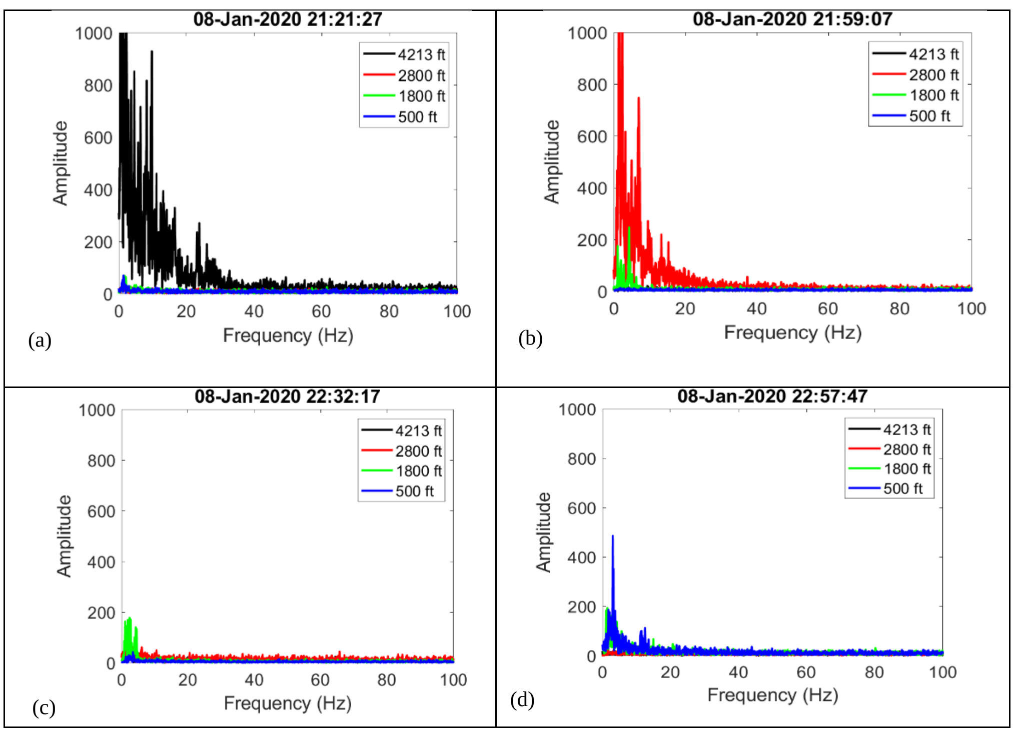

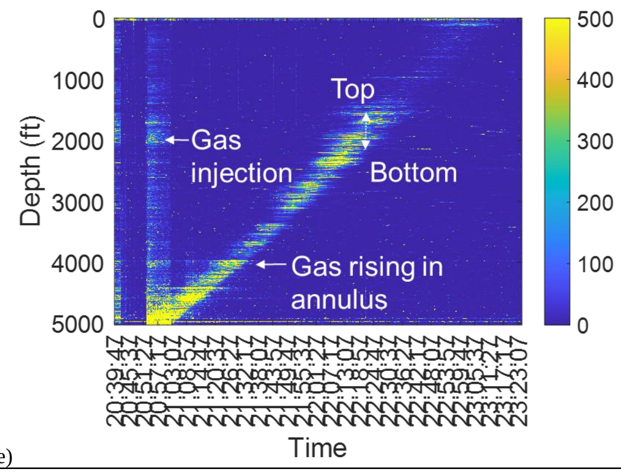

(e)

Fig. 4. (a-d) Spectral signatures of the gas migration in the annulus at different time instances as a function of depths. (e) DAS FBE for frequency band 10 to 50 Hz for Trial-1 showing clear gas signature.

4.2 Trial-2

The raw DAS strain rate data for Trial-2 was previously shown in Fig. 2b. Since the gas signature was buried in the background noise generated from the pump and water circulation, additional signal processing was necessary to optimize gas detection. To this end, techniques (a) through (d) describe in Sec. 3 were implemented on the DAS data with a time frame (or frame size) of 10 seconds and gauge length of 4.92 m (fixed in the interrogator). The resulting mean, standard deviation, RMS, and FBE (10-50 Hz) profiles are shown in Fig. 5. In all the mentioned profiles, gas migration signature is still buried in the severe pump noise and cannot be easily identified. Hence, additional signal conditioning needs to be deployed to optimize gas detection.

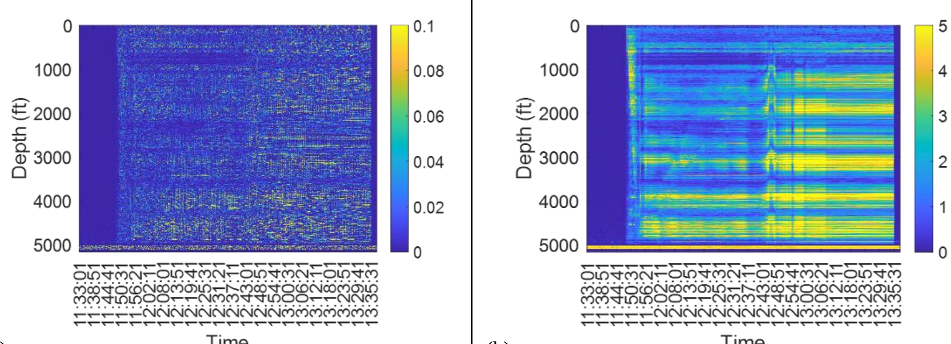

(a) (b)

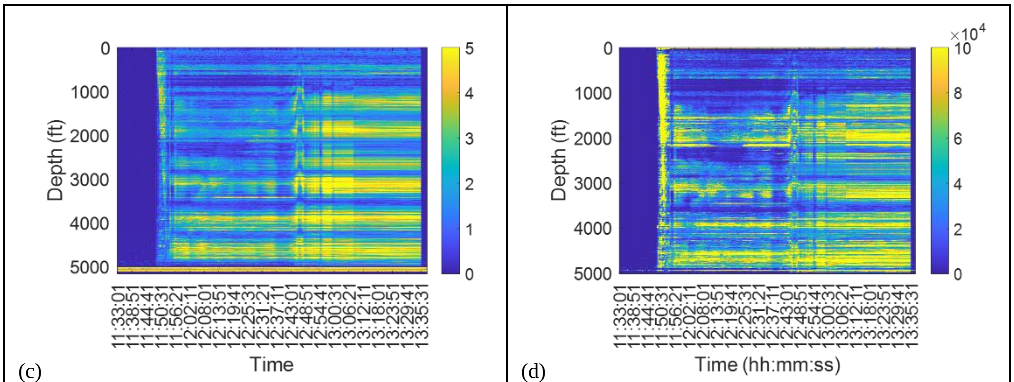

Fig. 5. Processed DAS data for Trial-2 using (a) mean (b) standard deviation (c) RMS (d) FBE.

As a next step, feature extraction techniques described in (e) through (g) in Sec. 3 were implemented on the DAS FBE profile. A 2-D FFT filter was used to remove the horizontal and vertical bands in the FBE, and the resultant signal is shown in Fig. 6a. The top and bottom edges of the gas slug region can be identified as the two diagonal lines which are highlighted in Fig. 6, which represent the gas slug migrating up the annulus. GBDIA is deployed on the FBE as the second technique to filter the horizontal components in the Fourier space and which are then converted back to the space and time domain. The signature of the gas rise event and the top and bottom of the gas slug are clearly visible as highlighted in Fig. 6b. The final technique is computing a gradient of the FBE data with respect to the time axis to filter out the horizontal bands. The filtered signal is shown in Fig. 6c which clearly shows the top and bottom ends of the migrating gas slug region. The results indicate that the feature extraction techniques were successful in removing the background noise and highlighting the gas rise signature. For the Trial-2 data, GBDIA and gradient filtering seem to outperform the 2D-FFT Filter. However, this does not imply that 2D-FFT filtering is necessarily inferior to the other two. The performance of any algorithm largely depends on the signal quality and the feature of interest.

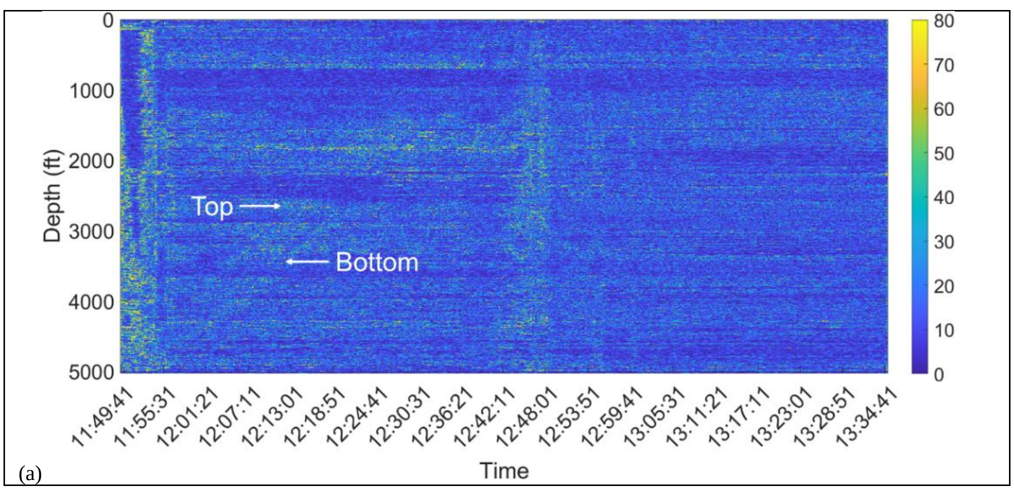

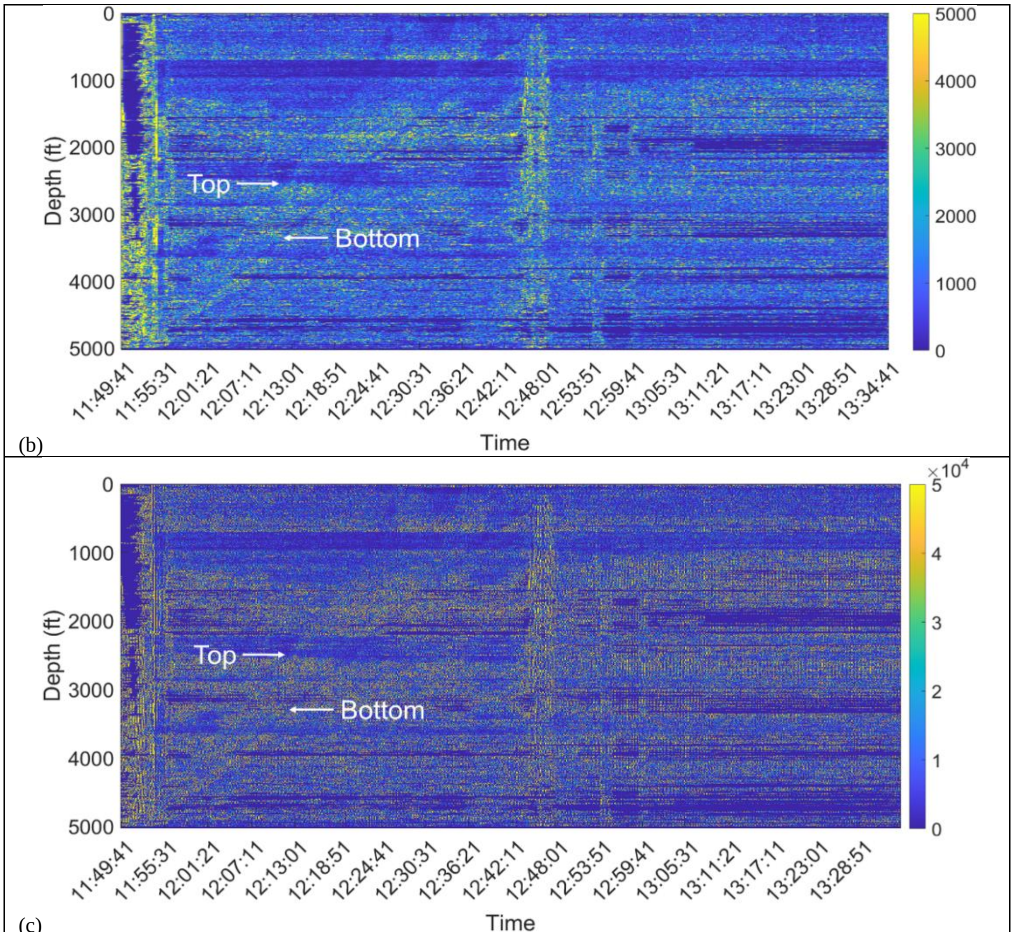

Fig 6. Filtered DAS FBE data for Trial-2 using (a) 2D-FFT (b) GBDIA (c) higher-order gradient filter.

4.3 Trial-3

In Trial-3, a relatively large gas slug volume of 80 bbl was injected at the top of the annulus and bullheaded down at a rate of 250 gpm. The resulting DAS strain rate data (shown previously in Fig. 1c) did not clearly display the gas signature due to the high background noise resulting from continuous fluid circulation. To optimize gas detection, the DAS strain rate data was processed using mean, standard deviation, RMS, and FBE and the results are displayed in Fig. 7. These profiles were generated using a time frame of 10 seconds and gauge length of 4.9 m. All the resulting profiles were noisy and only the top of the gas slug is easily visible.

In order to extract the signature corresponding to the bottom of the gas slug, gradient filtering was deployed as a feature extraction technique on all the profiles shown in Fig. 7. The gradient-filtered profiles of mean, standard deviation, RMS, and FBE are shown in Fig. 8. It can be observed that all the filtered profiles further enhance the top of the gas slug, however not significantly the bottom edge. A faint bottom edge is visible at shallower depths in Fig. 8a corresponding to the mean profile. The results necessitated another level of signal conditioning was needed to enhance the detection of the bottom of the gas slug region. Detection of both the top and bottom of the gas region is necessary for understanding the changing slug lengths and the full dynamics of gas displacement to decide the proper well control strategy. Further feature extraction was implemented on the FBE profile generated at 10-50 Hz frequency range as it inherently selects the desired frequency bins for optimized gas detection and isolates the unnecessary frequency components. Gradient filter followed by vertical GBDIA was implemented on the FBE profile and the result is shown in Fig 9. Here we can identify both the top and bottom of the gas slug, especially at the deeper depths, relatively more clearly.

The above analysis shows that the effectiveness of the filtering and feature extraction techniques depends on the signal of interest and also the level of noise present in the data. A combination of techniques may be needed in some cases to highlight the desired features. All the proposed signal conditioning techniques are computationally inexpensive and able to extract the key features for real-time data processing and low-latency visualization of the gas migration signatures in the wellbore in the presence of high background noise.

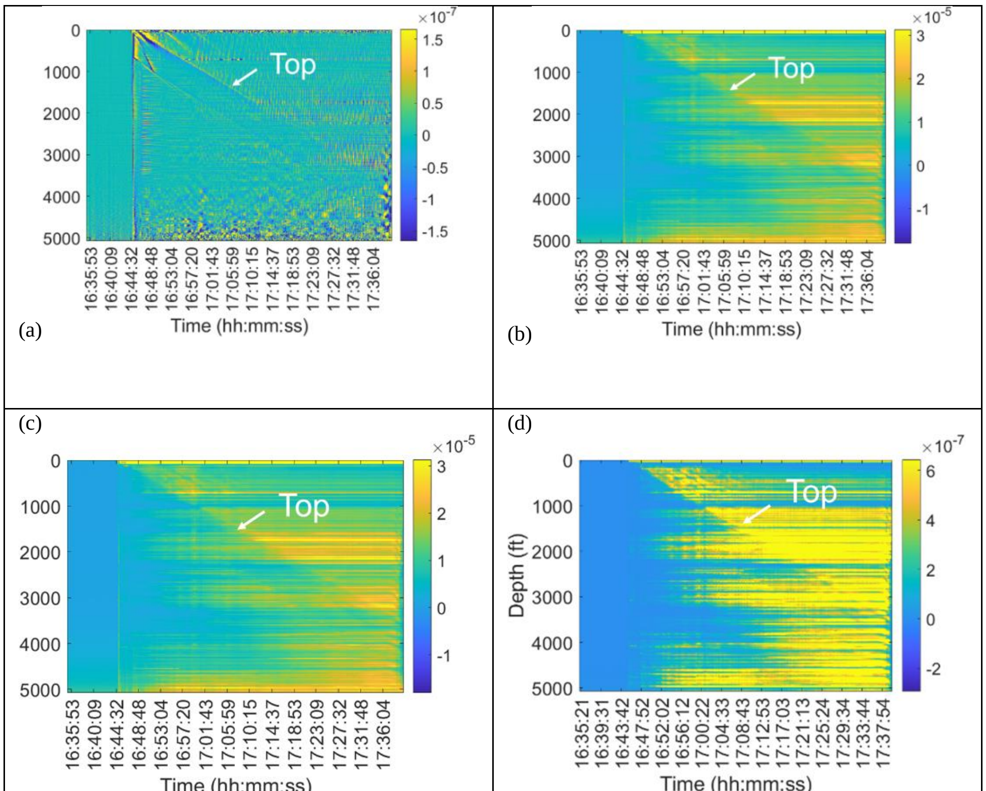

Fig 7. Processed DAS data for Trial-3 using: (a) Mean (b) Standard deviation (c) RMS (d) FBE (10-50 Hz).

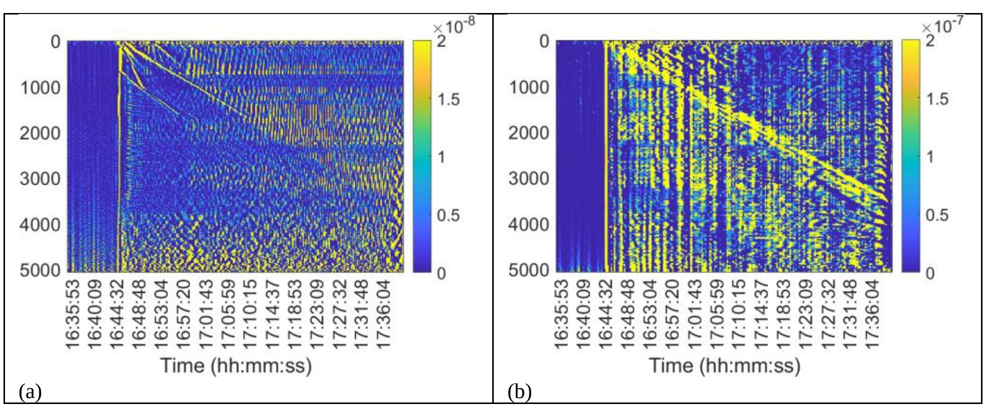

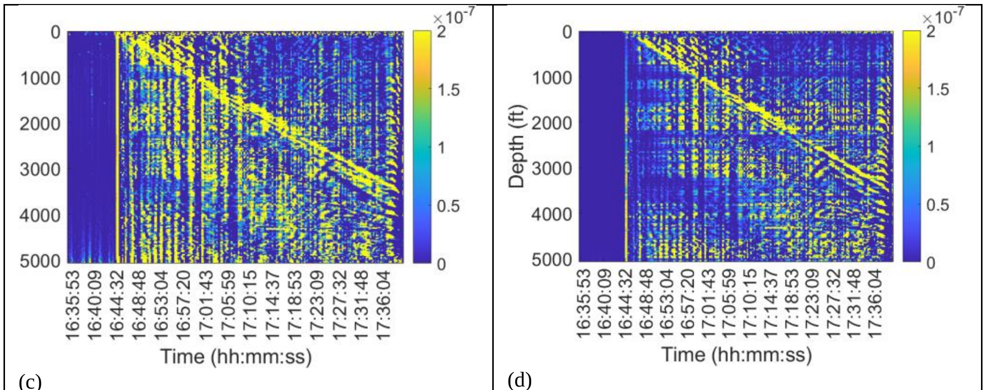

Fig. 8. Gradient filtered profiles for Trial-3 for the (a) mean (b) standard deviation (c) RMS (d) FBE.

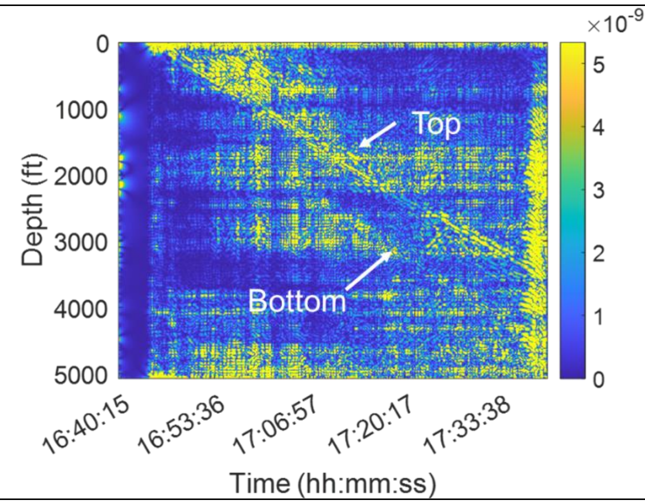

Fig. 9: Gradient and vertical GBDIA implemented on the DAS FBE for Trial-3.

So far, we have discussed the performance of different filtering and feature extraction techniques. However, DAS signal quality also depends on the frame size and gauge length of the acquisition that determine the temporal and spatial resolution of the DAS data, respectively. The sensitivity of these parameters is demonstrated on the DAS data acquired during Trial-3. In the first case, the FBE profile corresponding to 10-50 Hz frequency range is computed by fixing the gauge length at 4.9 m and varying the time frame of the raw DAS strain from 1 s to 30 s. Then the gradient filter is deployed as a feature extraction technique and the results of the filtered FBE are shown in Fig 10. Here we can observe that if the time frame is very small, the desired feature does not have enough energy to be contrasted from the background. This can be observed in Fig. 10a where the time frame of 1 s was used, and the resulting gas feature cannot be separated from the background even after the implementation of the feature extraction technique. As the time frame increases, the gas feature is more clearly visible, however the tradeoff is the contrast of the feature from the background. On the other hand, a smaller time frame leads to poor sharpness of the feature. Hence an optimum timeframe needs to be selected to improve the detection of the feature of interest.

The quality of FBEs with different frame rates are also quantified using the perception-based image quality evaluator (PIQE) score [14]. The PIQE score for an input image, in our case the DAS plots, is returned as a non-negative scalar between 0 and 100. The PIQE score is the no-reference image quality score. It has an inverse relationship with how good an image looks to the human eye. High perceptual quality is shown by a low score value, whereas a high score value implies poor perceptual quality. In Fig. 12a, the PIQE score is generated for images of random noise and filtered FBEs with various time frames for comparison. The PIQE scores indicate that the largest time frame and smallest time frame rates result in poor picture quality and among the time frames compared, 10 s seems to show the best outcome.

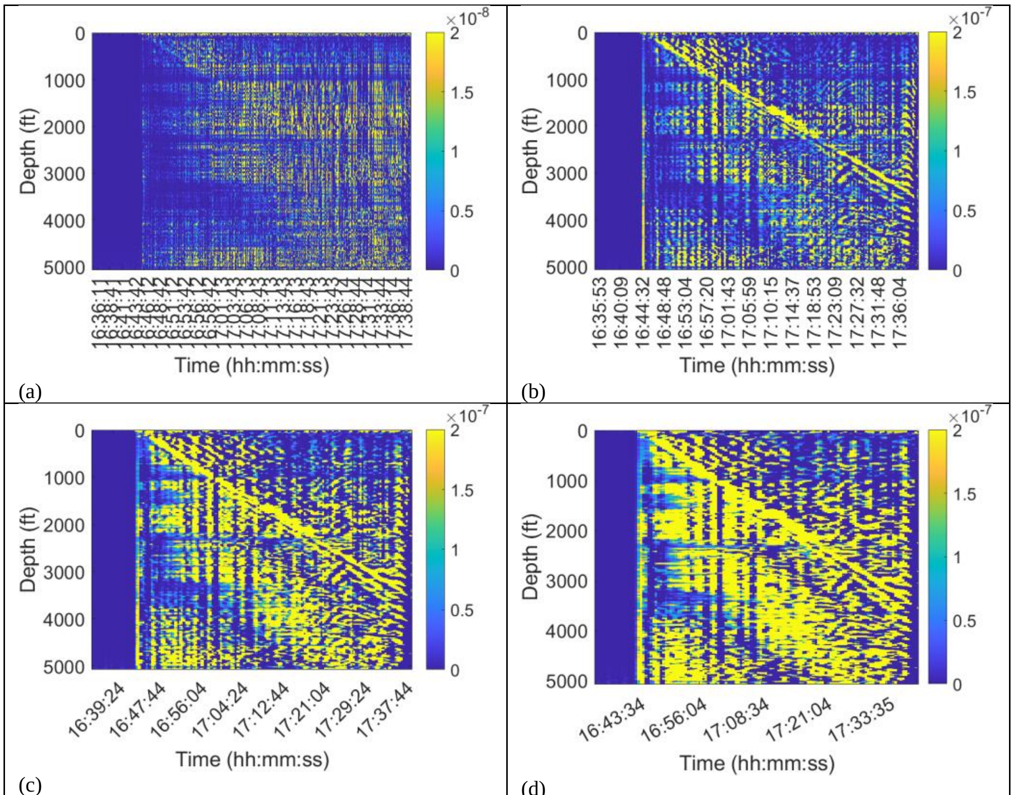

Fig. 10. FBE gradient of Trial-3 corresponding to frame size of (a) 1 s (b) 10 s (c) 20 s and (d) 30 s

Likewise, the effect of gauge length on the quality of DAS data and the ability to detect gas signatures was also investigated. Different gauge lengths were selected with respect to the incident laser pulse width used in the optical interrogator unit. The gradient-filtered FBE for different gauge lengths are plotted in Fig 11. Visually, we can observe that as the gauge length increases, the noise in the image appears to reduce, however, it is also fading the desired gas feature. Again, the quality of the image is quantified using the PIQE score and plotted in Fig. 12b which shows that as gauge length increases, image quality reduces. Based on this assessment, we can observe that the gauge length corresponding to the incident laser pulse width gives the best quality of the gas signature in the case we have analyzed.

Here the PIQE score is presented as one of the many available quantification tools to evaluate the image quality, which worked satisfactorily for the data presented. However, ultimately the ability to optimally detect the feature of interest will depend on the signal being monitored. Therefore, a single quantification parameter (such as PIQE) may not meet the needs of all applications for measuring signal quality.

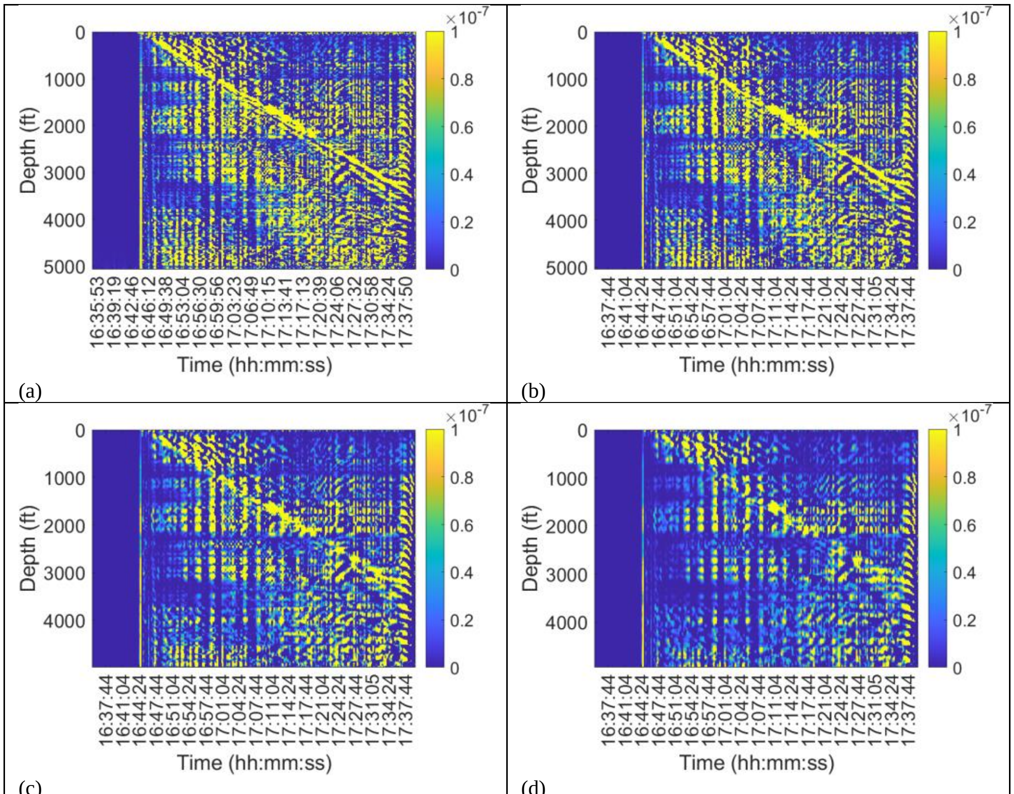

Fig. 11. Gradient of FBE for gauge length equal to the (a) incident pulse width (b)3X (c)6X and (d)9X pulse width.

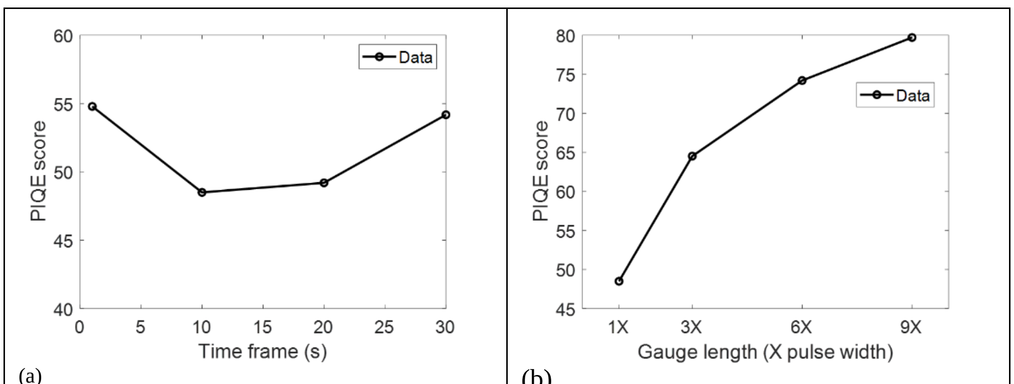

Fig. 12. PIQE score as a function of (a) time frame (b) gauge length.

4. Conclusions

This study demonstrates the application of optical fiber-based DAS for monitoring gas signature in a 5163 ft-deep wellbore. A suite of computationally inexpensive signal processing techniques were implemented on the DAS datasets acquired during multiphase flow experiments to optimize the detection of gas slug in the well in real time, with low latency. The proposed denoising techniques include both simple approaches, such as mean, standard deviation, RMS, and FBE estimation, as well as more involved filtering and signal conditioning using 2D-FFT filtering, GBDIA, and higher-order gradients. One or more of these methods can be implemented depending on the level of noise present in the data. The proposed techniques not only helped to enhance the gas signal but also reduced the DAS data size which can further help in optimizing the data storage and archival needs. The selection of the optimum frequency range corresponding to the gas rise signature using DAS spectrums is presented. The proposed techniques were able to extract the top and bottom edges of the gas slug feature in the wellbore despite the high noise present due to the fluid circulation and pumping. This work also discusses the effect of DAS acquisition parameters, such as the frame size and gauge length, on the visibility of the feature of interest.

5. Acknowledgements

The authors would like to thank the National Academies of Sciences' Gulf Research Program and ExxonMobil Research and Engineering Company for providing funds to support this research. The authors would also like to thank all collaborators who participated in the experiments at LSU. We are grateful for the inputs from the fiber-optic service providers, Schlumberger (Toba Ogunsanwo, Devin Paulk, and Mary Taylor) and Terra15 (Michael Roelens, Albert Carmenate, and Nader Issa). Some of this work has been presented at the Optical Fiber Sensors Conference (OFS-27), Virgina, USA, 2022

6. References

1. K. Johannessen, B. Drakeley , and M. Farhadiroushan, " Distributed acoustic sensing-a new way of listening to your well/reservoir." In SPE Intelligent Energy International. OnePetro (2012, March)
2. A. H. Hartog, Optical Fibre Sensors in the Oil, Gas and Geothermal Energy Extraction, (Optical Society of America, 2014).
3. M. M Molenaar, D. J .Hill, P. Webster, E. Fidan, and B. Birch. "First downhole application of distributed acoustic sensing for hydraulic-fracturing monitoring and diagnostics." SPE Drilling & Completion, *27*(01), 32-38 (2012).
4. J Sharma, O. L. Santos, G. Feo, O. Ogunsanwo, and W. Williams. "Well-scale multiphase flow characterization and validation using distributed fiber-optic sensors for gas kick monitoring." Optics Express, 28(26), 38773-38787 (2020)..
5. D. H. S. Group, "Final Report on the Investigation of the Macondo Well Blowout," Berkeley, USA (2011).
6. Y. Xu, Z. Guan, andW. Chen, "Methods of Early Gas Kick Detection andWell Control Risk Assessment in Deepwater Drilling," in SPE International Conference and Exhibition on Health, Safety, Security, Environment, and Social Responsibility (Abu Dhabi, UAE, 2018).
7. G. Feo, J Sharma, D. Kortukov, W. Williams, and T. Ogunsanwo." Application of distributed fiber optics sensing technology for real-time gas kick detection." In SPE Annual Technical Conference and Exhibition. OnePetro.(September 2019)
8. G. Feo, J Sharma, D. Kortukov, W. Williams, and T. Ogunsanwo. " Distributed fiber optic sensing for real-time monitoring of gas in riser during offshore drilling." Sensors, 20(1), 267 (2020)
9. O.L. Santos, W.C Williams,J. Sharma, M.A. Almeida, M.K. Kunju, and C.E. Taylor. " Use of Fiber-Optic Information To Detect and Investigate the Gas-in-Riser Phenomenon." SPE Drilling & Completion, 36(04), 798-815.(2021)
10. Terra 15. " Treble Dashboard user manual ." May 2022
11. J. Sharma, T. Cuny, O. Ogunsanwo, O. Santos." Low-frequency distributed acoustic sensing for early gas detection in a wellbore." IEEE Sensors Journal, 21(5), 6158-6169 (2020).
12. K. Chen, D. Zhu, and A. D. Hill."Acoustic signature of flow from a fractured wellbore." In SPE Annual Technical Conference and Exhibition. OnePetro. (2015, September).
13. Bouali, "A simple and robust destriping algorithm for imaging spectrometers: application to modis data," San Diego, California, ASPRS 2010
14. Annual Conference N. Venkatanath, D. Praneeth, Bh. M. Chandrasekhar, S. S. Channappayya, and S. S. Medasani. "Blind Image Quality Evaluation Using Perception Based Features", In *Proceedings of the 21st National Conference on Communications (NCC).* Piscataway, NJ: IEEE, 2015.